Modulated Drug Release Using Iontophoresis through Heterogeneous Cation-Exchange Membranes: Membrane Preparation and Influence of Resin Cross-Linkage

Steven P. Schwendeman,† Gordon L. Amidon,† Mark E. Meyerhoff,‡ and Robert J. Levy*,†,§

College of Pharmacy, The University of Michigan, Ann Arbor, Michigan 48109-1065, Department of Chemistry, The University of Michigan, Ann Arbor, Michigan 48109-1055, and Department of Pediatrics, The University of Michigan, R-5014 Kresge II, Ann Arbor, Michigan 48109-0576

Received September 27, 1991; Revised Manuscript Received January 21, 1992

ABSTRACT: A modulated drug delivery method using iontophoresis through rate-limiting membranes was investigated. Heterogeneous cation-exchange membranes (HCMs) were prepared by levigating conditioned sulfonated polystyrene beads in silicone rubber. Transport of two salts, (±)-phenylpropanolamine (PPA) hydrochloride and NaCl, across the above HCMs was examined as a function of resin cross-linkage. After preconditioning the membranes, iontophoretic delivery of PPA from 0.01 M PPA into 0.01 M NaCl at 37 °C increased with applied current (2–20 $\mu A/cm^2$) and the steady-state delivery rate was enhanced as much as 9-fold relative to the zero current rate (4% resin cross-linkage). The permselectivity of the HCMs for PPA and Na^+ over Cl^- was nearly ideal under zero current conditions ($t_{PPA} > 0.91$, $t_{Na^+} > 0.96$). High membrane resistance was observed during transference of PPA relative to Na^+ for HCMs with a high degree of resin cross-linkage ($Rs_{PPA} = 580 \pm 20$ kΩ, $Rs_{Na^+} = 15 \pm 2$ kΩ, 12% resin cross-linkage), suggesting pore exclusion of PPA. A dimensionless transport model was developed based on the works of Schlögl[1] and Teorell.[2] Using the model and membrane potential measurements during ion transport, the delivery rates of PPA were predicted and the PPA–Na^+ selectivity coefficients were determined. The theoretical flux of PPA showed excellent correlation with the mean observed flux ($r = 0.95$, $p < 0.001$) and the model predicts that the HCMs are mildly selective for PPA over Na^+. The rate of delivery of PPA was controlled using membranes which are permselective for cations. Hence, HCMs of this kind may be useful in modulated controlled drug delivery devices.

Introduction

Several controlled release methods have been reported in which the rate of drug delivery can be modulated after delivery has been initiated. These methods include: release from magnetic bead-loaded ethylene–vinyl acetate matrices,[3] implantable mechanical drug pumps,[4] electrochemically loaded drug electrodes,[5] and drug delivery devices using ultrasound[6] and iontophoresis.[7-10] While the field of transdermal iontophoresis has expanded over the past 10 years, there has been much less investigation of iontophoresis from implantable delivery systems or other routes of administration.[11,12] By utilizing the developed technologies of ion transport and ion exchange, we have sought to develop rate-limiting membranes for the study of iontophoresis as a modulated release strategy.

A most important aspect in controlling iontophoretic drug delivery is to prepare a membrane which is rate-limiting; that is, the ion transport (particularly under diffusion conditions) is controlled by the membrane as opposed to the Nernst diffusion layers adjacent to the membrane's surfaces.[13] Membranes which are permselective for ionized drugs reduce the competition of extraneous ions.[14] Ion-exchange membranes provide a nonspecific type of permselectivity which is based purely on the charge of the therapeutic agent. We have considered membranes which are used for electrodialysis, such as Nafion,[15] but these membranes are not usually rate-limiting for the counterion (i.e., membrane resistance too low) when using dilute salts and a normal range of membrane thickness (<2 mm) which can be placed in between standard diffusion cells, such as Crown Glass cells (Crown Glass Co., Somerville, NJ).

Permselectivity of the membrane for the ionized drug is a second design objective for iontophoretic devices. Heterogeneous ion-exchange membranes that contain conductive resinous beads in an inert binder[16] are perhaps the most basic of membranes which fit the above two design criteria. In this case, the membrane resistance to counterion transport can be altered by varying the type of exchange material and the geometric aspects concerning the formation of the inert matrix. Variables such as fraction of ion exchanger loaded, ion-exchange bead particle size, and membrane thickness can affect the conducting clusters[17] of ion-exchange material and, thus, the resistance of the membrane. Therefore, the geometric and heterogeneous nature of such membranes addresses the first goal, membrane rate control, and the use of an ion exchanger as a conductive medium addresses the second, drug permselectivity.

The formulation and characterization of sulfonated polystyrene-type cation exchangers was thoroughly investigated during the 1950s.[18] The sulfonic acid moiety, which is the charged group attached to the styrene polymer backbone, remains completely ionized even under extremely acidic conditions (apparent $pK < 1$).[19] Therefore, this cation exchanger was the most logical choice for cationic drug delivery. In addition, silicone rubbers have been used previously as drug loaded controlled release matrices in our laboratory.[20] This material provides a strong, insulative, and biocompatible matrix for a heterogeneous cation-exchange membrane.[21] We have chosen (±)-phenylpropanolamine (PPA) hydrochloride as a model compound to be delivered through the membranes because it represents a typical hydrochloride salt of a low molecular weight weakly basic compound that is positively

* To whom correspondence should be addressed.
† College of Pharmacy.
‡ Department of Chemistry.
§ Department of Pediatrics.

0024-9297/92/2225-2531$03.00/0

charged and stable at neutral pH.

This paper summarizes our results with respect to (1) preparation of heterogeneous cation-exchange membranes (HCMs), (2) investigation of the influence of resin cross-linkage on the iontophoretic delivery of PPA through HCMs, (3) evaluation of the HCM permselectivity for cations and its selectivity for the model compound relative to Na^+, and (4) prediction of the delivery rate of PPA through the HCMs as a function of a constant current.

Theoretical Section

Definitions. We define the following reduced (or dimensionless) variables where subscripts refer to one of n univalent counterions[22] with a charge of z ($= \pm 1$) moving in an ion-exchange membrane:

$$\xi \equiv x/L \tag{1}$$

$$\eta \equiv \phi/[RT/(zF)] \tag{2}$$

$$c_i^* \equiv c_i/X \qquad i = 1, 2, ..., n \tag{3}$$

$$I^* \equiv I/(D_1XAF/L) \tag{4}$$

$$j_i^* \equiv j_i/(D_1X/L) \qquad i = 1, 2, ..., n \tag{5}$$

$$\gamma_i \equiv D_i/D_1 \qquad i = 2, 3, ..., n \tag{6}$$

where x (ξ), ϕ (η), c_i (c_i^*), I (I^*), and j_i (j_i^*) represent dimensional (reduced) position coordinate, electric potential, concentration of i in the membrane, current, and unidirectional flux of ion i, respectively. γ_i is the reduced diffusion coefficient of counterion i. L and A are the thickness and surface area of the membrane. R, T, and F are the universal gas constant, absolute temperature, and Faraday's constant, respectively. X is chosen as the concentration of the fixed charge groups (normalized for membrane water volume). D_i and D_1 are the effective self-diffusion coefficients of counterion i and a reference counterion (denoted as 1) in the membrane.

We make the assumption, as described by Morf,[23] that when the membrane is originally in equilibrium with identical salt solutions, the two Donnan potentials cancel at the two solution/membrane interfaces (boundary potential, ϕ_b, is zero), and thus, the resistance of the membrane in the presence of counterion i is simply

$$Rs_i \equiv \phi_m/I = (RT/F)[L/(D_iXAF)] \qquad i = 1, 2, ..., n \tag{7}$$

where ϕ_m is the measured membrane potential with a positive potential causing a positive current (I).

We further assume that the thickness (L) and area (A) of the membrane are independent of the ionic form and that the concentration of the fixed charge groups (X) is the same in the presence of all counterions. Then, from the resistance of the membrane in the presence of counterion i and the reference counterion, Rs_i and Rs_1, I^*, j_i^*, and γ_i can be rewritten as

$$I^* = I/[RT/(FRs_1)], \tag{8}$$

$$j_i^* = (j_iA)/[RT/(F^2Rs_1)] \qquad i = 1, 2, ..., n \tag{9}$$

and

$$\gamma_i = Rs_1/Rs_i \qquad i = 2, 3, ..., n \tag{10}$$

Therefore, under the above assumption, only the resistance of the membranes to one reference counterion need be measured in order to convert the above dimensional variables into reduced form. In addition, the reduced diffusion coefficient of i becomes equivalent to the reduced conductance (reciprocal of resistance) of the membrane to i when the assumption of independence of counterion form is valid.

The molar selectivity coefficient for counterion i over the reference counterion is[24]

$$K^i_1 \equiv (c_iC_1)/(C_ic_1) \qquad i = 2, 3, ..., n \tag{11}$$

where C_i and C_1 are external concentrations of i and 1 exclusively in equilibrium with the ion exchanger and c_i and c_1 are concentrations of the two univalent counterions present in the membrane.

Dimensionless Model for a Bi-ionic System. Since we are interested in the case where a cationic drug, phenylpropanolamine (PPA), is delivered into NaCl, we consider only two counterions, hydrated PPA and Na^+. Because of its biological importance, and the previous literature on the transport of Na^+ in ion-exchange resins,[18] we choose Na^+ as the reference counterion (subscript 1), and PPA is then assigned subscript 2.

The general solution of steady-state Nernst–Planck equations[1,2] for $n = 2$ and $z = 1$, as described in the Appendix, gives the following from (A4) through (A7):[57]

$$Y = k_1e^{s\xi} + I^*/s \tag{12}$$

$$c_2^* = k_2e^{s\xi} + j_2^*/(\gamma s) \tag{13}$$

where the integration constants, k_1, k_2, I^*, and j_2^*, may be evaluated from the following boundary conditions (counterions are on opposing sides of the membrane):

$$\xi = 0 \qquad c_1^* = 0, c_2^* = 1, \text{ and } Y = \gamma \tag{14}$$

$$\xi = 1 \qquad c_1^* = 1, c_2^* = 0, \text{ and } Y = 1 \tag{15}$$

From (12) through (15), the integration constants are written as a function of the reduced electric field (s):

$$k_1(s) = (1 - \gamma)/(e^s - 1) \tag{16}$$

$$k_2(s) = -1/(e^s - 1) \tag{17}$$

and

$$I^*(s) = s(\gamma e^s - 1)/(e^s - 1) \tag{18}$$

$$j_2^*(s) = \gamma s e^s/(e^s - 1) \tag{19}$$

From the parametric solution, (18) and (19), where s is the parameter, the reduced flux (j_2^*) can be predicted by reduced current (I^*) and reduced PPA conductance (γ). The resulting reduced concentration profile of PPA from (13), (17), and (19) is

$$c_2^*(s,\xi) = (e^s - e^{s\xi})/(e^s - 1) \tag{20}$$

The membrane potential is the sum of the potential drop across the membrane and the boundary potential (assumed independent of s), which in reduced form gives ($\eta \equiv 0$ in the reference counterion reservoir)

$$\eta_m(s) = \int_1^0 (d\eta/d\xi)\, d\xi + \eta_b = s + \eta_b \tag{21}$$

The transference number of PPA, $t_2(s)$, can be obtained

from (j_2^*/I^*) by using (18) and (19):

$$t_2(s) = \gamma e^s/(\gamma e^s - 1) \quad (22)$$

and the enhancement function,[25] $E(s)$, defined as $j_2^*(s)/j_2^*(I^*=0)$, can be derived by noting that $s = -\ln \gamma$ when $I^* = 0$ (see (18)), and using (19) gives

$$E(s) = [(\gamma - 1)/(\ln \gamma)][(se^s)/(e^s - 1)] \quad (23)$$

Implicit in the use of the Nernst–Planck equation to describe the flux of each counterion is assumption of the independence of counterion activity coefficients with respect to position.[29] In this case, the molar selectivity coefficient for PPA over Na^+ can be related to the reduced boundary potential, η_b, as follows:[30]

$$K^2_1 = e^{-\eta_b} \quad (24)$$

In using the above relationship (24), similarly to relating reduced conductance to reduced diffusion coefficient, we must assume that the concentration of fixed membrane charge groups (X) is constant independent of counterion form.

Experimental Section

Materials. Unless otherwise stated, all chemicals were used as received. NaCl and (±)-phenylpropanolamine hydrochloride (MW of hydrochloride = 188) were obtained from Sigma (St. Louis, MO), and KCl was purchased from Mallinckrodt (Paris, KY). All aqueous solutions were prepared with distilled and deionized water (>16 MΩ·cm, Millipore Co., Bedford, MA). For membrane preparation, Silastic Q7-4840 (A/B) medical-grade silicone rubber was generously provided by Dow Corning (Midland, MI), and all Dowex 50W cation-exchange resin was obtained from Sigma. Silver wire (26 gauge, 0.405-mm diameter, 99.9% purity) and hydrochloric acid (Mallinckrodt) were used in preparation of Ag/AgCl electrodes. Agar (purified grade), used to prepare salt bridges, was from Fisher Scientific (Fairlawn, NJ). High performance liquid chromatography (HPLC) grade methanol (Mallinckrodt), glacial acetic acid (Baker Chemical, Phillipsburg, NJ), and 1-heptanesulfonic acid (Sigma) were used for HPLC.

Potentiometric and iontophoretic studies were carried out in Crown Glass side-by-side diffusion cells (3.4 mL/half-cell), Crown Glass Co. (Somerville, NJ). The temperature of the cells was maintained at 37 ± 1 °C by a Lauda thermostat (type K2-D), Messgerate-Werk Lauda, Inc. (Germany). Current was supplied by a galvanostat which was built by the Chemistry Electronics Shop at the University of Michigan. The 10-channel constant current source (current range: 0.67 to >1000 μA, 35-V maximum) supplied a current from 0.80 to 60 μA to the external electrolytic cell to within ±5% the desired current setpoint. Membrane potential was monitored with a digital multimeter, Fluke Mfg. Co. (Everett, WA), Model 8062A. For anodization of silver wire, platinum foil was required as a nonerodible electrode material, and a power supply (Bio Rad Laboratories, Model 500, Melville, NY) was used to drive the electrolytic current. A Virtis Freeze Dryer (No. 10-010, Gardiner, NY) was used to lyophilize the wet cation exchanger beads following conditioning. A caliper (Mitutoyo, No. 193-11, Japan) was required for determination of HCM thickness.

The HPLC system consisted of a Waters Pump (Model M6000A) and WISP autoinjector (Model 712) (Millipore Corp., Milford, MA), a Kratos variable UV detector (No. 783, Ramsey, NJ), and a Hewlett-Packard 3390A integrator (Avondale, PA).

Methods. Before use, all cation-exchange resin (Dowex 50W, X2, X4, X8, and X12, H^+ form, 200–400 mesh) was conditioned to remove impurities during manufacture. The procedure used was similar to that suggested by Helfferich.[31] The resin (30–60 g) was placed in a Buchner funnel and washed with alternating 300-mL volumes of 1 N NaOH and 1 N HCl (NaOH first). The cycle was repeated six times followed by six washes (300 mL/each) of 1 M NaCl in order to convert the resin into Na^+ form. The resin was then rinsed with distilled water repeatedly until the pH of the filtrate was the same as the distilled water. The wet resin was freeze-dried overnight and stored under reduced pressure in the presence of silica gel. Percent resin cross-linkage (or percent divinylbenzene content) was assumed as advertised by the manufacturer.[32]

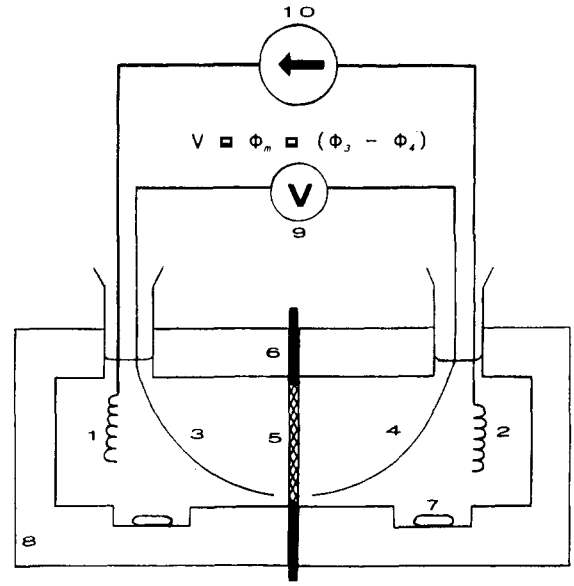

Figure 1. Schematic representation of apparatus used for iontophoretic studies. Constant current is driven by a 10-channel galvanostat (10) through two Ag/AgCl electrodes (1 and 2). Membrane potential (ϕ_m) is monitored by using a digital multimeter (9) and two reference Ag/AgCl electrodes (3 and 4) placed adjacent to the membrane surfaces. The membrane is composed of a silicone rubber–ion-exchange resin suspension (HCM) (5) in contact with salt solutions and pure silicone rubber (6) in contact with the diffusion cells. A temperature of 37 ± 1 °C is maintained by constant temperature bath (8), and solutions are mixed by magnetic stirring bars (7).

Membranes were prepared by mixing the dry conditioned resin, 42% by weight, with the prevulcanized form of the Silastic Q7-4840 part A/B mixture. The resulting suspension was placed in a mold under vacuum trap until bubbling. The mold was put under 1000 lbs of force in a Carver Press (Carver Inc., Menomonee Falls, WI) for 15 min and then set in the oven at 80 °C for 90 min. The resulting film was cut into a circular or square HCM, weighed, and the dry thickness measured with a caliper. For measurement of equilibrium water content, the membranes were placed in 0.01 M NaCl at 37 °C for 48 h (control experiments showed that equilibrium was reached shortly after 1 day), and the wet weight was recorded.

For potentiometric and iontophoretic studies the HCMs were modified to avoid membrane permeability changes caused by the diffusion cell/membrane interface.[33,34] Both faces of 420 ± 20 μm HCMs (0.36–0.40 cm^2) were covered with Teflon Overlay (Cole-Parmer, Chicago, IL) in order to maintain the HCM transport surface while leaving the edges exposed. The covered films were placed in the mold already containing the pure silicone polymer in prevulcanized form. The HCM/silicone rubber membrane was compression molded and vulcanized as previously discussed. After vulcanization, the exposed edge of the film had reacted with the silicone rubber to form a continuous membrane, and the Teflon Overlay was removed. This procedure eliminated any contact between the cation-exchange surface and the diffusion cell (see Figure 1). Before use, the above membranes were allowed to reach equilibrium in 0.01 M NaCl for 2 days in 37 °C and then were conditioned with current passage in the same salt (with frequent reservoir replacement) for 1 day at 20 μA/cm^2. The preconditioning was performed in order to remove any salts deposited during the silicone rubber vulcanization.

In preparation of the electrodes for current passage (electrodes 1 and 2, see Figure 1), silver wire was coiled around a glass rod and then anodized in 1 N HCl at ~0.4 mA/cm^2 for 4 h. In the electrochemical preparation, platinum foil formed the cathode and the voltage of the a power supply was adjusted periodically

to maintain the current setpoint. The reference Ag/AgCl electrodes (electrodes 3 and 4) for measurement of membrane potential were anodized uncoiled in the same manner, except using a 1-h duration since little AgCl was required. After anodization of the reference electrodes, a tightly fitting piece of Teflon tubing was placed around the wire so that only the ends of the wire were uncovered. The Teflon tubing served to insulate the reference electrodes from the electrodes for current passage in the crowded diffusion cell.

Before the measurement of the HCM resistance to Na^+ and PPA transference, the membrane was converted to the appropriate counterion form. This was achieved by placing the desired chloride salt (0.01 M) in both donor and receiver half-cells and initiating a current density of 20 $\mu A/cm^2$ (with periodic solution replacement) until the membrane potential had stabilized for a few hours. The membrane potential was measured in the presence of each of the 0.01 M salts at 0, ±5, ±10, ±20, and ±40 μA for Na^+ and 0, ±0.8, ±2, ±4, and ±8 μA for PPA. There was roughly a 5-min period between each measurement. The resistance of the membrane in the presence of each salt was calculated as the slope of the linear regression fit to the potential versus current data ($r^2 > 0.99$).

Iontophoretic delivery of PPA from 0.01 M PPA into 0.01 M NaCl was carried out for 0, 2, 5, 10, and 20 $\mu A/cm^2$. The experimental configuration is shown in Figure 1. The above concentrations were sufficiently dilute for maintenance of the Donnan exclusion of Cl^- [35] and sufficiently concentrated so that large concentration changes would not occur between sampling. At each time point, the entire volume of the receiver half-cell (containing the cathode) was sampled, the donor reservoir (containing the anode) was removed, and both half-cells were rinsed with distilled water. The half-cell contents were each replaced with 3 mL of the appropriate salt solution, and the experiment was continued. The membrane potential was measured at this time because the concentration of Cl^- was the same in both half-cells so that the reference electrode potentials would (virtually) cancel. Currents were varied in descending order beginning with 20 $\mu A/cm^2$. For the voltage–current characteristic, additional current setpoints were used (including negative current values) without sampling for PPA.

The effect of Na^+ and PPA activity on the zero current membrane potential was determined for a salt concentration range of 10^{-4}–10^{-1} M. Before the experiment, the membrane was converted into the appropriate counterion form. The first Ag/AgCl reference electrode (electrode 3, see Figure 1) was placed in the left half-cell (37 °C) containing 0.01 M of the chloride salt solution, which remained constant throughout the experiment. The second reference electrode (electrode 4) was placed in a stirred beaker (at room temperature) containing 0.01 M of the same salt solution. The beaker solution and the right half-cell were interposed with a salt bridge (2% Agar in 1 M KCl). This configuration allowed for the maintenance of all electrode and junction potentials while the concentration of salt in the right half-cell was varied. Sign convention of the membrane potential was the same as in Figure 1 ($\phi_3 - \phi_4$). Activity coefficients were calculated by using the extended Debye–Hückel equations[36] with characteristic hydrated diameters of 0.40 and 0.90 nm for the Na^+ and PPA hydrated cations, respectively.

PPA was analyzed by high-performance liquid chromatography with UV detection at 256 nm. Similar assays have been reported.[37,38] The column was a 15-cm μ-Bondapak C-18 and reverse phase. The mobile phase consisted of 47% methanol, 52% water, 1% glacial acetic acid, and 0.005 M 1-heptanesulfonic acid as an ion-pairing agent.

Data Analysis. In order to predict the steady-state flux of PPA (j_2) from a constant current (I), the reduced current (I^*) was first calculated from mean experimental values of γ and Rs_1 by (8). The parameter s was obtained from the resulting I^*, (18), and a root-finding method (such as the half-interval method). The reduced PPA flux (j_2^*) was obtained from s by means of (19), and the PPA flux was deduced with (9).

The selectivity coefficient of the membranes for PPA over Na^+ was obtained by two methods. In method I, the limiting case of the model at zero current was utilized. Since $s = -\ln \gamma$ when I (or I^*) = 0, the reduced boundary potential (η_b) was related to the reduced membrane potential (η_m) and reduced PPA conductance (γ) under zero current conditions (from (21)) by using mean experimental values for η_m and γ:

$$\eta_b = \eta_m(I^*=0) + \ln \gamma \tag{25}$$

The PPA–Na^+ selectivity coefficient (K^2_1) was related to η_b by (24).

Equations 18 and 21 can be combined and written in the following form:

$$I^*(\eta_m) = \frac{(\eta_m - \eta_b)(\gamma e^{\eta_m - \eta_b} - 1)}{e^{\eta_m - \eta_b} - 1} \tag{26}$$

In some cases, the measured membrane potential in the presence of a single counterion was found to become nonlinear above a certain constant current.[39] This voltage–current characteristic was adequately fit using the hyperbolic sine function such that

$$I = a \sinh^{-1}(\phi_m/b) \tag{27}$$

where a and b are constants. The above nonlinear behavior was encountered during iontophoresis of PPA into NaCl for the HCMs containing 2 and 4% resin cross-linkage. For these cases, the nonlinearity was compensated by an empirical relationship for $\gamma(\eta_m)$ consistent with (27) as follows:

$$\gamma(\eta_m) = A \sinh^{-1}[(\eta_m - \eta_b)/B]/(\eta_m - \eta_b) \quad \text{for } \eta_m > \eta_b$$
$$= A/B \quad \text{for } \eta_m \le \eta_b \tag{28}$$

The expression involving $\sinh^{-1}$ in (28) approaches A/B, the ratio of the two empirical constants, as $\eta_m \to \eta_b$. In method II, nonlinear regression (using the quasi-Newton method) of (26) only (when assuming constant γ) or (26) and (28) (when assuming nonlinear γ) to fit I^* versus η_m data yielded η_b and γ (or A and B for nonlinear γ). The PPA–Na^+ selectivity coefficient was then calculated as in method I by using η_b and (24).

Table I
Reduced PPA Conductance and Swelling Behavior of HCMs

resin cross-linkage (%)	dry surface area (cm^2)	Rs_1 (kohm)	Rs_2 (kohm)	γ (Rs_1/Rs_2)	fractional water content in NaCl
2	0.40[a]	2.3 ± 0.2[b]	7.6 ± 0.4	0.30 ± 0.01	0.529 ± 0.007
4	0.40	19 ± 3[c]	76 ● 11	0.25 ± 0.02	0.428 ± 0.005
8	0.40	7.3 ± 2.3	240 ± 40	0.030 ± 0.005	0.211 ± 0.003
12	0.36	15 ± 2	580 ± 20	0.026 ± 0.003	0.176 ± 0.004

[a] Surface area of membranes used during resistance measurement only. [b] Mean ± sem. [c] Membrane potentials for currents above 10 μA were omitted because nonlinear resistance was observed above this value.

Results

Resistance and Swelling Behavior. For constant surface area (0.36–0.40 cm^2), the mean resistance of the membranes to Na^+ transport, Rs_1, varied between 2.3 and 19 kΩ with no particular trend for the different cross-linked resins (Table I). In contrast, the resistance of the membranes in 0.01 M phenylpropanolamine (PPA) hydrochloride, Rs_2, increased nearly 2 orders of magnitude as cross-linkage of the resin loaded was increased from 2 to 12%. Since the resistance to transport of the two cations is dependent not only on the resin type but also on the heterogeneity and geometry of the membrane, the reduced conductance of PPA, γ ($\equiv Rs_1/Rs_2$), was calculated; the resulting values are listed in Table I. The values of γ decreased with increased cross-linkage with a particularly sharp cut-off between 4 and 8%. The water content of the membranes exhibited a trend similar to the decline in reduced PPA conductance, suggesting that the resistance behavior is influenced by the amount of water in the membrane.

Steady-State Iontophoretic Delivery of PPA. Over the current range (0–20 $\mu A/cm^2$), significant increases in

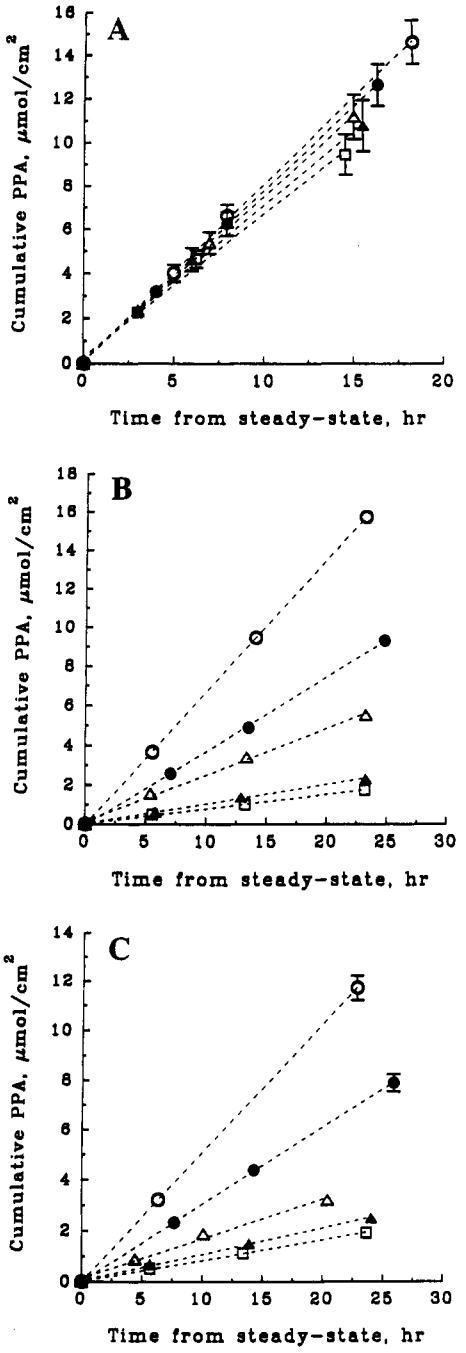

Figure 2. Iontophoretic delivery of phenylpropanolamine (PPA) hydrochloride from 0.01 M PPA into 0.01 M NaCl through HCMs having 2% (A, $n = 3$), 4% (B, $n = 4$), and 8% (C, $n = 3$) resin cross-linkage. Cumulative mass of PPA after the system had reached a steady-state is plotted versus time from steady-state for □, 0; ▲, 2; △, 5; ●, 10; and ○, 20 μA/cm² input current density. Data represents mean ± sem. Error bars not shown when smaller than symbols.

delivery rate were observed (Figure 2) as applied current was increased for the HCMs with the higher resin cross-linkage (4 and 8%), although only marginal increased delivery rate with increased current was observed for the HCMs with resin of lower divinylbenzene content (2%). Before the potentiometric and iontophoretic experiments, the membranes were equilibrated for 2 days at 37 °C and current conditioned at 20 μA/cm² in 0.01 M NaCl for 1 day. During iontophoresis from 0.01 M PPA into 0.01 M NaCl the delivery rate of PPA was enhanced as much as 9-fold relative to the zero current rate (4% cross-linkage).

Zero Current Response to Counterion Activity. The zero current transference numbers of Na^+ and PPA, t_1 and t_2, respectively, were found to be greater than 0.91 for all the membrane types. The zero current membrane potential response to changes in Na^+ and PPA activity (product of counterion concentration (M) and activity coefficient) is displayed in Figure 3. This experiment is analogous to the calibration curve for a pH electrode. The slopes of the membrane potential versus logarithm of counterion activity are listed in Table II, and the corresponding zero current transference numbers were calculated by assuming position independence.[40] A Nernstian response ($2.3RT/F = 61.5$ mV/decade log counterion activity) or perfect Donnan exclusion of Cl^- was observed within experimental error for the HCMs with 4% resin cross-linkage or greater. Sub-Nernstian behavior was observed for HCMs with 2% divinylbenzene content owing to a decreased Donnan potential as the concentration of fixed sulfonic acid groups decreases with increasing HCM water content.[35] The response over the lowest decade of log concentration range (10^{-4}–10^{-3} M) was not considered since

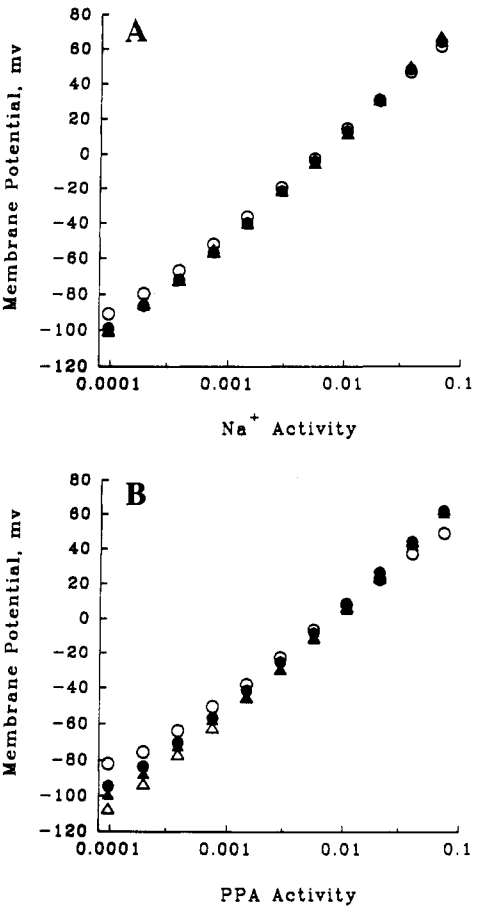

Figure 3. Potentiometric evaluation of membrane permselectivity for cations. Zero current membrane potential is plotted versus activity of Na^+ (A) and PPA (B) for ○, 2% ($n = 3$); ●, 4% ($n = 2$); △, 8% ($n = 3$); and ▲, 12% ($n = 3$) resin cross-linkage. Data represent mean values, and standard error bars were smaller than symbols.

Table II
Potentiometric Determination of HCM Permselectivity for Cations

resin cross-linkage (%)	$d\phi_m/d \log (a_1)$ (mV/decade)	t_1	$d\phi_m/d \log (a_2)$ (mV/decade)	t_2
2	57.1 ± 0.3[a]	0.96[b]	50.5 ± 0.4	0.91
4	60.3 ± 0.3	0.99	59.1 ± 0.6	0.98
8	61.0 ± 0.7	1.0	62 ± 1	1.0
12	62.1 ± 0.9	1.0	60 ± 1	0.99

[a] Mean ± sem. [b] $t_i = [1 + d\phi_m/d \log (a_i)/(2.3RT/F)]/2$, $i = 1, 2$.

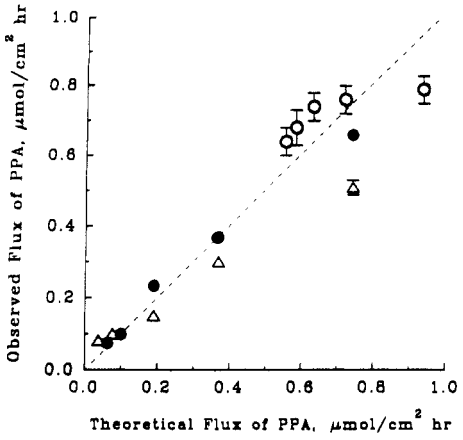

Figure 4. Prediction of steady-state iontophoretic delivery of PPA. Observed flux (mean ± sem) is plotted versus theoretical flux, which was determined by the model and resistance data from Table I for ○, 2%; ●, 4%; and △, 8% resin cross-linkage. The dashed line illustrates where theoretical and observed flux coincide. Error bars not shown when smaller than symbols.

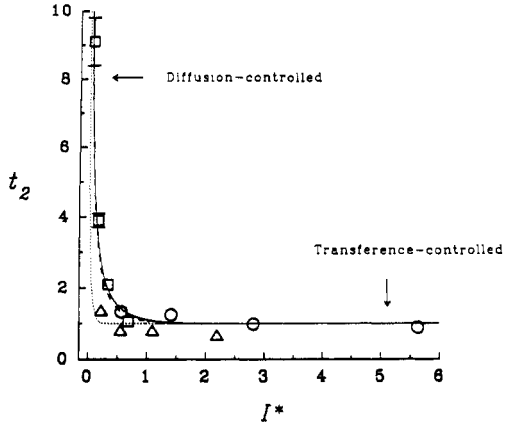

Figure 5. Depiction of the transition of the transport behavior from electrodiffusion to ionic transference mechanisms. Transference number of PPA (t_2) during iontophoretic delivery is plotted verus reduced current (I^*) for □ and —, 2%; ○ and - - -, 4%; and △ and · · ·, 8% resin cross-linkage. Symbols represent experimental data (mean ± sem), and lines were predicted by the model. Error bars not shown when smaller than symbols.

anomalous effects such as diffusion from the salt bridge are thought to be present in this region.

Theoretical Evaluation of the Flux of PPA. There was in general excellent agreement ($r = 0.95$, $p < 0.001$) between the observed steady-state flux of PPA versus the theoretical flux predicted by the model (Figure 4). The theoretical flux of PPA (steady state) was calculated from the mean Rs_1 and γ values listed in Table I and (8), (9), (18), and (19), as described in Data Analysis. There appears to be good accuracy when predicting the flux for the 2 and 4% cross-linked HCMs (<25% error[41]), but the zero current flux for the 8% cross-linked HCM was not adequately estimated by the model (120% error). The deviation of the predicted from observed flux for the HCM with the higher cross-linkage suggests some nonideal transport behavior of PPA in this membrane type.

The transition of the transport mechanism[42] from electrodiffusion to ionic transference during iontophoretic delivery of PPA can be evaluated from Figure 5, where the transference number of PPA, t_2, from the steady-state data and the theoretical model are plotted versus reduced current, I^* (constant current normalized for membrane resistance to Na^+), for the various membrane types. At very low I^*, the transference number of PPA approaches infinity since the flux of PPA is essentially constant and changes in I^* only slightly perturb the counter-diffusion of PPA and Na^+. When I^* is very high, the theoretical transference number of PPA approaches one, and thus, the flux of PPA is linearly proportional to the input current according to Faraday's law.

Efficiency of the Delivery of PPA during Iontophoresis. No information about the permselectivity during ionic transference can be derived from these data for the 2% cross-linked HCM (Figure 5). The 20 $\mu A/cm^2$ (equivalent to the largest I^* for each membrane type) transference number for this membrane was greater than 1 (1.06 ± 0.05), indicating partial diffusion control. The mean transference numbers of PPA for the 4 and 8% cross-linked HCMs at 20 $\mu A/cm^2$ were 0.68 and 0.90, respectively, illustrating that the HCMs are highly permselective for PPA over Cl^- during ionic transference. The above values do indicate, however, that there is additional Cl^- transport (and reduced efficiency) when the current is turned on, since the transference number of PPA under zero current conditions (see Table II) was always greater than 0.98 for these two membrane types.

Nonlinear Regression of the Reduced Voltage–Current Characteristic. Measured values for γ (Table I) were in excellent agreement with the γ and limiting γ ($= A/B$) values that were determined by nonlinear regression using the reduced voltage–current data during iontophoretic delivery of PPA (Table III). Figure 6 depicts the voltage–current characteristic for individual membranes where (1) the system had attained a steady-state, and (2) prior to the delivery experiments, the resistance of each HCM was measured in the presence of dilute NaCl. In the figure, the reduced membrane potential, η_m (membrane potential divided by 26.7 mV), is plotted against a broad range of reduced current, I^*, which includes negative current values. The result of the nonlinear regression of (26) and (28) using the $\eta_m - I^*$ data are also plotted in Figure 6, and the parameters are listed in Table III. The model appears to describe the voltage–current behavior adequately, although there is some variability in the data at high reduced current. The regression parameters which are listed in Table III consist of the reduced PPA conductance, γ (assumed constant for the 8% cross-linked HCM and dependent on η_m for the HCMs with 2 and 4% resin cross-linkage), and the boundary potential, η_b (assumed constant). The mean values of γ and limiting γ ($= A/B$) produced by nonlinear regression (and from Table I) were 0.43 (0.30), 0.26 (0.25), and 0.034 (0.030) for 2, 4, and 8% cross-linked HCMs, respectively, further indicating the integral role of the reduced PPA conductance in the bi-ionic system.

Determination of HCM Selectivity Coefficient. The determined PPA–Na^+ selectivity coefficients (K^2_1) were all greater than 1, indicating that the HCMs have a higher affinity for PPA than for Na^+ (Table III). In addition, an apparent trend of increased selectivity for PPA over Na^+ was observed as resin cross-linkage was increased. The boundary potential (η_b) was obtained from the zero current membrane potential during counter-diffusion of PPA and Na^+ using (25) (method I) or from the nonlinear regression described above during iontophoresis of PPA into NaCl (method II). The selectivity coefficient, K^2_1, was calculated from η_b using (24).

Discussion

Iontophoretic Delivery of PPA. The prediction of iontophoretic drug delivery rate is important for the design of membranes for iontophoretic delivery devices. Using

Table III
Determination of PPA–Na^+ Selectivity Coefficient

resin cross-linkage (%)	$\eta_m(I^* = 0)$	η_b	K^2_1 (method I)	nonlinear regression of I^* vs η_m				K^2_1 (method II)
				A	B	γ or A/B	η_b	
2	0.60 ± 0.01[a]	−0.60	1.8	2.6 ± 0.4[b]	6.0 ± 1.6	0.43	−0.23 ± 0.22	1.3
4	0.44 ± 0.02	−0.95	2.6	2.6 ± 0.4[b]	9.9 ± 2.5	0.26	−0.62 ± 0.22	1.9
8	0.69 ± 0.01	−2.8	16			0.034 ± 0.003[c]	−2.7 ± 0.3	15

[a] Mean ± sem. [b] Inverse hyperbolic sine function used for γ. [c] Constant value used for γ.

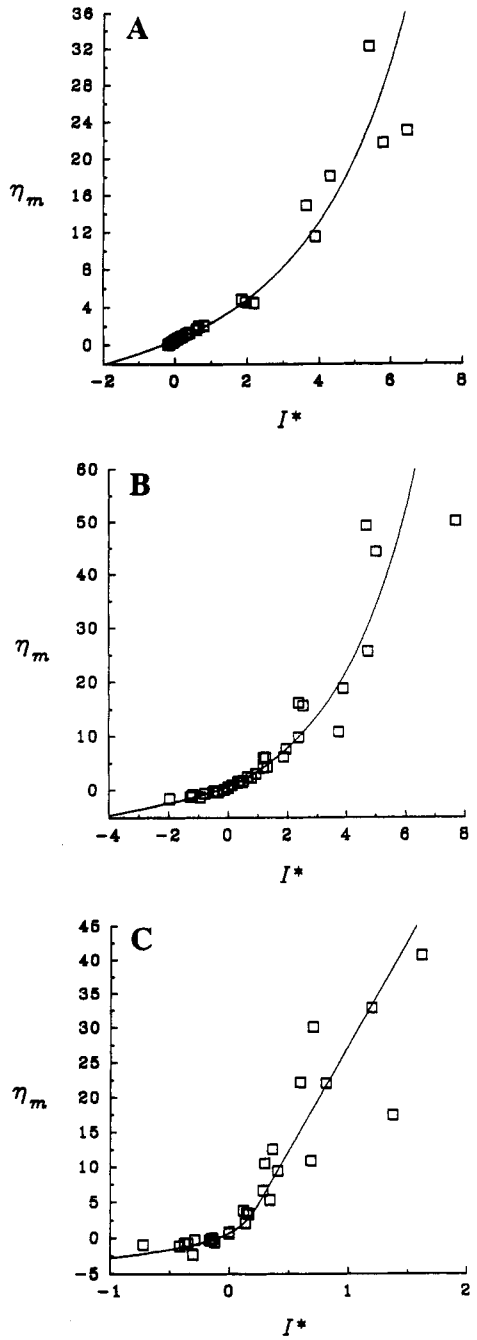

Figure 6. Reduced voltage–current characteristic for membranes having 2% (A, n = 3), 4% (B, n = 6), and 8% (C, n = 6) resin cross-linkage. Reduced membrane potential (η_m) at steady-state is plotted versus reduced current (I^*) for current density range of −5 to 20 $\mu A/cm^2$ (4 and 8% cross-linked HCMs) and −5 to 225 $\mu A/cm^2$ (2% cross-linked HCMs). □ represent experimental data for individual membranes and — the best fit line.

simple measurements such as membrane sodium resistance, Rs_1, and reduced conductance of PPA, γ (see Table I), a fairly accurate estimate of flux during iontophoresis can be obtained, as in Figure 4. Since the membranes with 8% resin cross-linkage are believed to exclude PPA (mean γ = 0.030), the assumption of equal concentration of counterions in the membrane (see Theoretical Section) would not be valid. This may explain the inability of the model to predict the steady-state flux of PPA at zero or low current for this membrane. The mechanistic reason for the observed differences in iontophoretic enhancement (see Figure 2) are illustrated in the transition from diffusion to transference-controlled behavior (see Figure 5). Since the current interval chosen (0–20 $\mu A/cm^2$) was in the region of partial diffusion-control for the 2% cross-linked HCM, no significant increase in delivery rate was observed as current was increased. A greater current would have been required in order to achieve greater enhancement of delivery rate. However, the current interval for both the 4 and 8% cross-linked HCMs extended well into the transference-controlled region, and therefore, significant increases in delivery rate relative to the zero current rate were observed. The reduced current at which the theoretical curves in Figure 5 converge to a transference number of one ($I^* \sim 1.5$ for the 2 and 4% HCMs) has added significance. This is the current where all counter-diffusion of Na^+ (diffusion against the current) is theoretically turned off. If it were desirable to avoid diffusion of external cations into an iontophoretic device, this current could be maintained with a minimal increase in basal delivery rate.

Membrane Resistance and the Pore Exclusion of PPA. The absence of any trend of the membrane resistance in the presence of Na^+, Rs_1, with varied resin cross-linkage (see Table I) is not necessarily of any mechanistic importance. The resistance to ion transport is expected to be determined by conduction through (and perhaps around) the resin beads and by the connectivity (or percolation) of the resinous phase through the silicone rubber matrix.[43] The latter phenomenon, which may explain the variable resistance to Na^+, is a complex issue which is currently under investigation.[39] On the other hand, the reduced conductance of PPA, γ, should not be biased by the percolation of the resin through the silicone rubber since both cations (Na^+ and PPA) cannot penetrate the rubber, which can be considered a perfect insulator. The most general effect of an increase in resin cross-linkage is the resultant decrease in membrane water content. The insulating silicone rubber absorbs negligible water;[44] therefore, a decrease in water content will be accompanied by a smaller pore size within the resin bead.

The trend of decreased reduced PPA conductance as the cross-linkage is increased is consistent with the concept of increased friction of PPA relative to Na^+ within the pores. In particular, the sharp decline of resistance ratio between 4 and 8% resin cross-linkage appears to indicate a cut-off in which the pores inside the resin beads are excluding the larger PPA molecule. It is likely that the PPA transport observed through the HCMs with the highly cross-linked beads is occurring around the bead rather than through the bead as intended. This may explain the negligible change in γ between the 8 and 12% cross-linked HCMs.

Size exclusion of quaternary ammonium ions in sulfonated polystyrene resin beads has been reported by

Hale,[45] where a decrease in exchange capacity for the organic cations was observed relative to ammonium ion as resin cross-linkage and size of the cation was increased. In this previous study, tetraethylammonium ion (MW = 130), which has similar molecular weight to PPA (MW = 153), was found to have 87% of the exchange capacity as compared to ammonium ion for resin with 5% divinylbenzene (DVB) content and 63% of the total capacity for resin with 10% DVB content. Since only partial exclusion would be necessary to severely restrict the transport through the resin bead, the above reported change in exchange capacity for tetraethylammonium ion is believed by the authors to be consistent with the above values for reduced conductance of PPA (where Na^+ is the reference nonexcluded cation).

HCM Permselectivity for Cations. The potentiometric evaluation of the membrane for cations is a simple and useful method for evaluating the manufacture of the membrane. The membranes studied were all greater than 96% permselective for Na^+ over Cl^- (see Table II) and greater than 91% permselective for PPA. The permselectivity evaluated under zero current conditions supports our view that the HCMs constitute an integral membrane system. If a defect (a hole for example) were large enough to allow significant transport, the above response to changes in counterion activity would not reflect ideal permselectivity for the cation since Cl^- would be free to transport across the neutral pore. The permselectivity of PPA during transference (see Figure 5) was less than the zero current permselectivity for the 4 and 8% cross-linked HCMs, which suggests that the Donnan equilibrium at the solution/membrane interface becomes less efficient as current is increased.

Membrane Potential during Iontophoresis of PPA. The membrane potential, apart from its link to selectivity coefficient, is important when considering the power consumption of the iontophoretic delivery device. In Figure 6, the voltage–current characteristic is illustrated using reduced variables such that there is no bias for the membrane heterogeneity. The nonlinear behavior recorded for the 2 and 4% cross-linked HCMs may be a result of several factors. One explanation is the concentration polarization at the solution/membrane interface, which would increase with increased applied current. Although this effect should cause a nonlinear resistance, the effect should not be dependent on the cross-linkage of the membrane. A more probable explanation is that there is a constriction in the connectivity of the resin beads through the silicone rubber. This issue has been discussed by Siegel.[46] In control experiments,[47] the current at which nonlinear resistance occurs is highly dependent on resin loading, supporting this notion. Yet another explanation may be the presence of convective mass transport, the discussion of which is to follow. Unexpectedly, the voltage–current characteristic for the membranes with 8% resin cross-linkage was fit adequately by the model using a constant γ.

The similarity between the values of γ and (A/B) obtained from the I^*–η_m nonlinear regression (Table III) and the directly measured γ values (Table I) indicates a redundancy of the two measurements. The former measurement is preferred, since the measured membrane potential during iontophoresis of PPA into NaCl allows also the estimate of the PPA–Na^+ selectivity coefficient.

HCM Selectivity for PPA over Na^+. In the bi-ionic system (PPA–Na^+) investigated, the selectivity coefficient is not required for prediction of delivery rate. However, if it were to become desirable to incorporate an additional extraneous counterion into the drug reservoir, the general solution in the Appendix could be used for $n = 3$, and the selectivity coefficient between the extraneous counterion and the drug would be inserted in the boundary conditions required to derive the solution. The two methods used in the determination of the selectivity coefficient (see Table III) yielded similar values. Method I has the advantage of simplicity, and method II has the advantage of representing more data. The greater selectivity of the HCMs for PPA over Na^+ is consistent with the decreased free energy from hydrophobic bonding and van der Waal's interaction between PPA and the polystyrene backbone of the ion-exchange resin.[48] The selectivity of the 8% cross-linked HCM for PPA over Na^+ is considered to be artificially high since the definition of selectivity coefficient is also dependent on the equal exchange capacity of counterions assumption (see Theoretical Section). One may actually expect that these membranes would prefer Na^+ over PPA since selectivity in resins of high cross-linkage has been shown to be strongly dependent on swelling pressure,[49] where the resin prefers the smaller hydrated counterion. Hence, the measured selectivity coefficient for the HCM with 8% cross-linkage is considered to be biased by the pore exclusion of PPA.

Applications of Iontophoresis to Modulated Controlled Release. Complications resulting from cardiac arrhythmias continue to claim hundreds of thousands of lives each year. Advantages of local epicardial administration of antiarrhythmics has been discussed previously.[50] Iontophoresis of what are usually weakly basic compounds would allow the delivery of the antiarrhythmic agent to be turned on in a life-threatening moment. This general concept of detection/response is currently in practice using the implantable defibrillator systems.[51]

Several aspects of the iontophoretic system make this modulated release strategy attractive. The power requirement of a modulated device would be small since excess energy is not lost moving the solvent or generating heat. This would allow a device to be implanted for extended time periods in a self-contained manner using the same battery similar to cardiac pacemakers. This is in contrast to modulated systems which require large external electromagnets[3] or ultrasonic generators[6] and implantable drug pumps,[4] whose battery life-time is limited. An iontophoretic system could be constructed to be small enough to be implanted in a large number of sites in the body. A basic system would require only a rate-limiting membrane, a battery and control circuitry, a reservoir filled with drug solution, and internal and external microelectrodes.

Like the previously mentioned modulated delivery systems, iontophoretic systems can produce a broad range of zero-order delivery rates (we report 9-fold in our simplified system). A device based on electrolyte transfer through a "charged" membrane could conceivably produce an infinite number of delivery patterns. Thus, unusual pulsatile hormonal secretions[52] might be emulated using this modulated technique. One can envisage a device constructed to release deficient neurotransmitters such as dopamine at levels (~pg/h) that have shown the ability to reverse the Parkinson-like effects in the apomorphine induced rotational rat model.[53] Miller[5] has been developing systems for electrochemical release from dopamine electrodes for the same purpose. Also, like the mechanical drug pumps, iontophoretic devices could be very useful in delivering anticancer agents directly to the infected tissue. Many of the compounds of interest (e.g., dopamine (MW = 154) and lidocaine (MW = 235)) are weakly

basic and roughly the same size as phenylpropanolamine (MW = 153). Therefore, the results for these compounds would be expected to be similar to those in this study, although experiments with dopamine must be carried out in an oxygen-free environment.

Iontophoretic systems that use rate-limiting membranes such as pHEMA (poly(hydroxyethyl methacrylate))[11] or agar and dialysis membranes[12] have recently been reported. These systems have achieved modulated delivery rates but with two distinctive disadvantages as compared to the system described here. The present system uses cation-exchange material, which is ideally permselective for cations (see Table II). Therefore, high efficiency of the delivery of the drug (and low power consumption) was achieved (see Figure 5). Using the "neutral" gel (contains no charged groups) pHEMA, an efficiency of less than 8%[11] was calculated based on delivery rates reported, although extraneous ions were present in the donor reservoir. Of perhaps equal importance is the inevitable depletion of the drug concentration in the drug reservoir with time. The distribution of the drug counterion into ion-exchange resins is quite indifferent to external drug concentration.[35] Thus, the boundary conditions given by (14) and (15) should be maintained (and delivery rate should remain unchanged) even if the drug solution were depleted to 10% of its original concentration. Distribution into a "neutral" gel would be expected to be highly dependent on external drug concentration, and thus, one would expect a change in delivery rate as the drug solution was depleted.

Nonideal Behavior (Electroosmosis and Electrolyte Sorption). In our theoretical treatment, we assumed the Nernst–Planck equation for the flux of the counterions, thus not taking into account any convective mass transport which may be present.[54] The importance of any convective transport mechanism (usually electroosmosis) becomes apparent when considering the power requirement and displacement of the solvent from the donor reservoir in an implantable iontophoretic delivery device. The most practical explanation for omission of any convective term is that "simplest is best". The flux of PPA for the low and zero current data was very accurately predicted by the model (particularly for 2 and 4% cross-linked HCMs); hence, the simple model without the convective term has utility in this regard. Even at higher current, one may not expect the transference number of PPA to be increased by convection (and thus become larger than one), particularly since PPA is the only counterion in the donor solution. The steady-state membrane potential may be a different matter entirely. The nonlinear resistance associated with PPA transference for the 2 and 4% cross-linked HCMs may be linked to convection. Since more energy would be exhausted by the system to move the solvent during convective mass transport, one would expect an increase in electrical resistance of the membrane. Schlögl[55] has suggested a rule of thumb water content (65%) for charged membranes, above which it becomes valuable to consider convection. This value is almost identical for the water content of the resinous phase of the 4% cross-linked HCM (64%), which supports the use of convective terms for both 2 and 4% cross-linked membranes when considering the voltage–current characteristic. The best method of measuring solvent movement is by monitoring solvent in an attached capillary.[56]

The concentration of the release vehicle (0.01 M NaCl) was chosen in order to maintain ideal Donnan exclusion of Cl^- (negligible electrolyte sorption) from the membrane. This strategy was successful at least under zero current conditions (see Table II). The next step would be to use a more realistic release vehicle such as an isotonic buffer. Under these more rigorous conditions, we will be able to associate any decrease in counterion transport, compared with our previous results, to Cl^- transport due to decreased Donnan potential or increased conductance of the film between the silicone rubber and the ion-exchange beads. Therefore, our present study represents a basic model which will help us gain insight into more complex systems.

Conclusions

A model bi-ionic system comprising the transport of phenylpropanolamine (PPA) and Na^+ through heterogeneous cation-exchange membranes (HCMs) was investigated to evaluate iontophroesis as a modulated release strategy. Rate-limiting HCMs can be prepared from a suspension of cation-exchange resin and silicone rubber. Modulated delivery rates of a model compound through these membranes are controlled by the input current. The cross-linkage of the resin controls the reduced PPA conductance and swelling of the membrane and restricts the size of the cationic drug transported. The membranes are permselective for PPA under diffusion and transference conditions. The theoretical model, which uses membrane potential measurements during ion transport, adequately describes the delivery rate and the voltage–current data in the bi-ionic system. Furthermore, the model predicts that the HCMs are mildly selective for PPA over Na^+. In summary, the above experimental and theoretical approaches may prove valuable for developing clinically useful iontophoretic release devices.

Acknowledgements. Financial support to S.P.S. was provided by the National Institutes of Health Pharmacological Track Training Grant (5-T32-GM-07767) and a Pharmaceutical Manufacturers Association Foundation Predoctoral Fellowship. This research was also supported in part by NIH Grant HL 41663 and an American Heart Association Established Investigatorship (R.J.L.). The authors would like to thank Dr. Weiliam Chen for his aid with illustrations.

Appendix

General Solution of Steady-State Nernst–Planck Equations for *n* Univalent Counterions with Charge *z* Moving in an Ion-Exchange Membrane. The steady-state Nernst–Planck equations for n counterions in dimensionless form are

$$j_1^* = -(dc_1^*/d\xi + c_1^* \, d\eta/d\xi) \qquad \text{(A1.1)}$$

$$j_2^* = -\gamma_2(dc_2^*/d\xi + c_2^* \, d\eta/d\xi) \qquad \text{(A1.2)}$$

$$\vdots \qquad \vdots$$

$$j_n^* = -\gamma_n(dc_n^*/d\xi + c_n^* \, d\eta/d\xi) \qquad \text{(A1.}n\text{)}$$

The condition of constant current is the following:

$$I^* = z(j_1^* + j_2^* + \ldots + j_n^*) \qquad \text{(A2)}$$

Assuming the constraint of charge neutrality between counterions and the univalent fixed charged groups

$$c_1^* + c_2^* + \ldots + c_n^* = 1 \qquad \text{(A3)}$$

By linear combination of (A1.1)–(A1.n), the general solution of (A1) with conditions (A2) and (A3) has been obtained by Schlögl[1] and by Teorell.[2] The result in

dimensionless form is given by

$$Y = k_1 e^{s\xi} + I^*/(zs) \quad \text{(A4)}$$

$$c_i^* = k_i e^{s\xi} + j_i^*/(\gamma_i s) \quad \text{for } i = 2, ..., n \quad \text{(A5)}$$

where k_i is the ith integration constant and Y and s are defined as follows:

$$Y \equiv c_1^* + \gamma_2 c_2^* + ... + \gamma_n c_n^* \quad \text{(A6)}$$

$$s \equiv -d\eta/d\xi = j_1^* + j_2^* \gamma_2^{-1} + ... + j_n^* \gamma_n^{-1} \quad (= \text{constant}) \quad \text{(A7)}$$

References and Notes

(1) Schlögl, R. *Z. Physik Chem. (Frankfort)* **1954**, *1*, 305–339.
(2) Teorell, T. *Z. Elektrochem.* **1951**, *55*, 460–469.
(3) Edelman, E. R.; Brown, L.; Taylor, J.; Langer, R. *J. Biomed. Mater. Res.* **1987**, *21*, 339–353.
(4) Heruth, K. T. *Ann. N. Y. Acad. Sci.* **1988**, *531*, 72–75.
(5) Miller, L. L.; Smith, G. A.; Chang, A. C.; Zhou, Q. X. *J. Controlled Release* **1987**, *6*, 293–296.
(6) Kost, J.; Leong, K.; Langer, R. *Proc. Nat. Acad. Sci. U.S.A.* **1989**, *86*, 7663–7666.
(7) Burnette, R. R.; Bagniefski, T. M. *J. Pharm. Sci.* **1988**, *77*, 492–497.
(8) Srinivasan, V.; Higuchi, W. I.; Su, M. H. *J. Controlled Release* **1989**, *10*, 157–165.
(9) Kasting, G. B.; Bowman, L. A. *Pharm. Res.* **1988**, *5*, 443–446.
(10) Padmanabhan, R. V.; Phipps, J. B.; Lattin, G. A. *J. Controlled Release* **1990**, *11*, 123–135.
(11) D'Emanuele, A.; Staniforth, J. N. *Pharm. Res.* **1991**, *8*, 913–918.
(12) Heil, R. W., Jr. *Proc. Intern. Symp. Controlled Release Bioact. Mater.* **1991**, *18*, 369–370.
(13) Helfferich, F. *Ion Exchange*; McGraw-Hill Book Company: New York, 1962; pp 348–349.
(14) Phipps, J. B.; Padmanabhan, R. V.; Lattin, G. A. *J. Pharm. Sci.* **1989**, *78*, 365–369.
(15) Narebska, A.; Koter, S.; Kujawski, W. *J. Memb. Sci.* **1985**, 153–170.
(16) Wyllie, M. R.; Patnode, H. W. *J. Phys. Chem.* **1950**, *54*, 204–227.
(17) Stauffer, D. *Introduction to Percolation Theory*; Taylor and Francis: Philadelphia, 1985; pp 15–58.
(18) Helfferich, F. *Ion Exchange*; McGraw-Hill Book Company: New York, 1962.
(19) Helfferich, F. *Ion Exchange*; McGraw-Hill Book Company: New York, 1962; p 86.
(20) Golomb, G.; Dixon, M.; Smith, M.; Schoen, F. J.; Levy, R. J. *J. Pharm. Sci.* **1987**, *76*, 271–276.
(21) Boretos, J. W. *Polym. Sci. Technol.* **1975**, *8*, 87–98.
(22) Counterions are ions with opposing charge to the charge of the fixed charged groups in the ion exchanger.
(23) Morf, W. E. *The Principles of Ion-selective Electrodes and of Membrane Transport*; Elsevier Scientific Publishing Company: New York, 1981; p 93.
(24) Helfferich, F. *Ion Exchange*; McGraw-Hill Book Company: New York, 1962, p 154.
(25) The definition of enhancement function is taken from previous works which discuss iontophoretic enhancement across the skin.[26-28]
(26) Kasting, G. B.; Keister, J. C. *J. Controlled Release* **1989**, *8*, 195–210.
(27) Pikal, M. J.; Shah, S. *Pharm. Res.* **1990**, *7*, 213–222.
(28) Srinivasan, V.; Higuchi, W. I.; Sims, S. M.; Ghanem, A. H.; Behl, C. R. *J. Pharm. Sci.* **1989**, *78*, 370–375.
(29) Helfferich, F. *Ion Exchange*; McGraw-Hill Book Company: New York, 1962, p 359.
(30) Helfferich, F. *Ion Exchange*; McGraw-Hill Book Company: New York, 1962, pp 154, 373, 381.
(31) Helfferich, F. *Ion Exchange*; McGraw-Hill Book Company: New York, 1962, p 230.
(32) *Dowex: Ion Exchange*; The Dow Chemical Company: Midland, MI, 1962; p 17.
(33) Brennen, K. R.; Hills, G. J. In *Biological Aspects of Electrochemistry*; Milazzo, G., Jones, P. E., Rampazzo, L., Eds.; Birkhäuser Verlag: Basel, 1971; pp 183–194.
(34) Burnette, R. R.; Ongpipattanakul, B. *J. Pharm. Sci.* **1988**, *77*, 132–137.
(35) Helfferich, F. *Ion Exchange*; McGraw-Hill Book Company: New York, 1962; pp 136–137.
(36) Bockris, J. O.; Reddy, A. K. N. *Modern Electrochemistry Vol. 1*; Plenum: New York; 1973; p 27.
(37) Shenoy, B. B.; Gupta, V. D. *J. Pharm. Sci.* **1984**, *62*, 802–804.
(38) Kou, J. Ph.D. Thesis, The University of Michigan, Ann Arbor, MI, 1987.
(39) Schwendeman, S. P.; Levy, R. J.; Murphy, H. A.; Amidon, G. L. *Pharm. Res.* **1991**, *8*, S-141.
(40) DeNuzzio, D.; Berner, B. *J. Controlled Release* **1990**, *11*, 105–112.
(41) Percent error is defined as $(j_2(theo) - j_2(expt)) \cdot 100\%/j_2(theo)$.
(42) Electrodiffusion is used to describe the transport due to both gradients of chemical (concentration) and electrical potential. Ionic transference is used to describe transport due to an electrical potential gradient only.
(43) Siegel, R. A.; Kost, J.; Langer, R. *J. Controlled Release* **1989**, *8*, 223–236.
(44) Golomb, G.; Fisher, P. *J. Controlled Release* **1990**, *12*, 121–132.
(45) Hale, D. K.; Packham, D. I.; Pepper, K. W. *J. Chem. Soc.* **1956**, 844–851.
(46) Siegel, R. A. In *Controlled Release of Drugs: Polymers and Aggregate Systems*; Rosoff, M., Ed.; VCH Publishers: New York, 1989; pp 17–21.
(47) Schwendeman, S. P., unpublished results.
(48) Helfferich, F. *Ion Exchange*; McGraw-Hill Book Company: New York, 1962, p 163.
(49) Helfferich, F. *Ion Exchange*; McGraw-Hill Book Company: New York, 1962, pp 158–159.
(50) Sintov, A.; Scott, W. A.; Siden, R.; Levy, R. J. *J. Cardiovas. Pharmacol.* **1990**, *16*, 812–817.
(51) Reid, P. R.; Mirowski, M.; Mower, M. M.; Platia, E. V.; Griffith, L. S.; Watkins, L., Jr.; Bach, S. M., Jr.; Imran, M.; Thomas, A. *Am. J. Cardiol.* **1983**, *51*, 1608–1613.
(52) Reiter, R. J.; Vaughan, M. K. *Ann. N.Y. Acad. Sci.* **1991**, *618*, 11–27.
(53) Becker, J. B.; Robinson, T. E.; Barton, P.; Sintov, A.; Siden, R.; Levy, R. J. *Brain Res.* **1990**, *508*, 60–64.
(54) Barry, P. H.; Hope, A. B. *Biophys. J.* **1969**, *9*, 700–728.
(55) Schlögl, R. *Discuss. Faraday Soc.* **1956**, *21*, 46–52.
(56) Pikal, M. J.; Shah, S. *Pharm. Res.* **1990**, *7*, 213–222.
(57) For two counterions we drop the subscript on γ_2, so the variable becomes γ.

Registry No. NaCl, 7647-14-5; Na, 7440-23-5; dowex 50W, 11114-15-1; dowex 50W-X2, 12612-37-2; dowex 50W-X4, 11113-61-4; dowex 50W-X8, 11119-67-8; dowex 50W-X12, 9056-03-5; (±)-phenylpropanolamine hydrochloride, 154-41-6.